A High Spectral Efficiency Coherent RoF System Based on OSSB Modulation With Low-Cost Free-Running Laser Sources for UDWDM-PONs

Xiang Chen, *Student Member, IEEE*, and Jianping Yao, *Fellow, IEEE, Fellow, OSA*

***Abstract*—A coherent radio over fiber (RoF) system based on optical single-sideband modulation with no optical carrier (OSSB) for ultradense wavelength division multiplexing passive optical networks (UDWDM-PONs) is proposed and experimentally demonstrated. For one channel of the UDWDM-PONs, at the transmitter, the OSSB RoF signal is generated using a dual parallel Mach–Zehnder modulator (DP-MZM) with a real-valued precoded microwave vector signal which is applied to the DP-MZM via the two electrodes with one having a 90° phase shift. Then, the OSSB RoF signal is sent to a coherent receiver over a single-mode fiber (SMF). The coherent receiver with a free-running laser source as a local oscillator (LO) is used to perform the coherent detection. To recover the standard microwave vector signals from the real-valued precoded microwave vector signal that is embedded in a strong phase noise introduced by both the transmitter laser source and the LO laser source, a digital signal processing algorithm is developed to perform phase noise cancellation. An experiment is performed. The transmission of a 1.25-Gbps quadrature phase shift keying, a 1.875-Gbps eight-phase shift keying (8-PSK), and a 2.5-Gbps 16 quadrature amplitude modulation (16-QAM) microwave vector signals with a channel spacing as narrow as 3 GHz over a 25-km SMF is experimentally demonstrated. For the transmission of the 2.5-Gbps 16-QAM microwave vector signal, the received optical sensitivity at forward error correction level over a 25-km SMF link is −24.8 dBm, while for the 1.875-Gbps 8-PSK microwave vector signal, it can reach −29.8 dBm which leaves an enough margin to accommodate the splitting losses in the optical distribution networks.**

***Index Terms*—Laser phase noise, optical coherent detection, optical single-sideband modulation with no optical carrier (OSSB), phase noise cancellation (PNC), radio over fiber (RoF), ultradense wavelength division multiplexing passive optical networks (UDWDM-PONs).**

I. Introduction

RADIO over fiber (RoF) is one of the promising last mile solutions for next generation broadband wireless access networks [1]–[3]. In recent years, RoF links based on optical double-sideband with carrier (ODSB+C) modulation and direct detection has been widely studied, since it is easy to implement and is less costly [1]–[3]. But such an optical modulation scheme makes poor use of the optical spectrum resources, since the spectrum between the two sidebands (the lower and upper sidebands) cannot be utilized effectively. In addition, the information carried by the upper sideband and lower sideband is exactly identical, thus the spectrum of one of the two bandwidths is completely wasted. To solve the problem, RoF links based on the optical single-sideband with carrier (OSSB+C) modulation employing direct detection have been widely studied. In addition to an increased spectral efficiency, the use of OSSB+C modulation can also avoid the power penalty resulted from the fiber chromatic dispersion [4]–[9]. For direct detection of an OSSB+C-modulated RoF signal, the optical carrier has to be preserved. However, the optical carrier actually does not carry any information and around 90% of the optical power is occupied by the optical carrier, which would decrease significantly the energy efficiency. Thus, OSSB modulation with fully suppressed optical carrier (OSSB) [10] or partially suppressed optical carrier [11] has been proposed to increase the energy efficiency. An RoF signal with a partially suppressed optical carrier has an improved energy efficiency, but the spectral efficiency is still poor. In addition, with a fully suppressed optical carrier, an RoF link becomes much less sensitive to fiber nonlinear effects, which is extremely attractive for ultra-dense wavelength division multiplexing (WDM) RoF passive optical networks (PONs) (UDWDM-RoF-PONs), a potential solution for the next generation broadband wireless access networks (e.g., 5G). In a UDWDM-RoF-PON, however, the channels are very tightly spaced with a channel spacing of 6.25 GHz or less, thus an effective use of the limited spectrum is particularly important. In addition, due to the tightly spaced channels, the use of a WDM filter may not be able to demultiplex the ultradense channels, thus direct detection with a WDM filter is not a feasible solution. To demultiplex the ultradense channels without the use of a WDM filter, one potential solution is to use coherent detection. Through coherent detection, the channels can be separated electronically in a coherent receiver. Furthermore, coherent detection can also provide high receiver sensitivity [12]–[14]. On the other hand, coherent detection is sensitive to the phase noise introduced by the transmitter and local oscillator (LO) laser sources. In addition, the unstable frequency difference between the transmitter laser source and LO laser source due to the frequency instability of the two laser sources must be cancelled, to effectively recover the OSSB RoF signal. In the past, optical phase-locked loop (PLL) was used to lock the frequency and the phase of the LO laser source to those of

Manuscript received November 16, 2015; revised February 20, 2016; accepted April 4, 2016. Date of publication April 4, 2016; date of current version April 30, 2016. This work was supported by the Natural Sciences and Engineering Research Council of Canada.

The authors are with the Microwave Photonics Research Laboratory, School of Electrical Engineering and Computer Science, University of Ottawa, Ottawa ON, K1N 6N5, Canada (e-mail: xchen134@uottawa.ca; jpyao@eecs.uOttawa.ca).

Color versions of one or more of the figures in this paper are available online at http://ieeexplore.ieee.org.

Digital Object Identifier 10.1109/JLT.2016.2550766

0733-8724 © 2016 IEEE. Personal use is permitted, but republication/redistribution requires IEEE permission.
See http://www.ieee.org/publications_standards/publications/rights/index.html for more information.

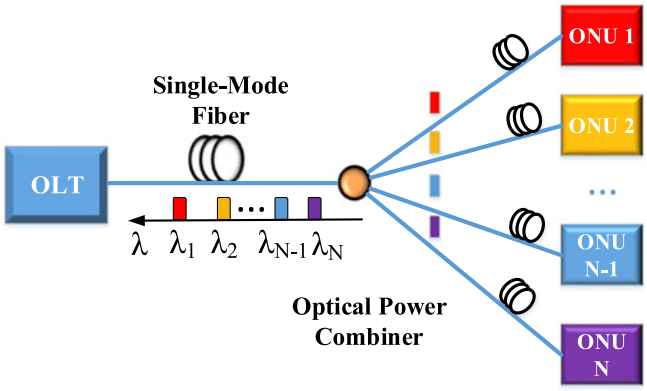

Fig. 1. The architecture of a UDWDM-PON. OLT: optical line terminal, ONU: optical network unit.

the transmitter laser source [15], which makes the scheme very complicated. Another way to eliminate the frequency difference and the phase noise is to use the optical coherent detection with differential detection in the electrical domain [16]. The limitation of this approach is that the RoF link is not transparent to the modulation format and the data rate. Besides, both the schemes are designed for optical baseband communication systems.

Fig. 1 shows the architecture of a coherent UDWDM-PON. Note that the usual wavelength multiplexer (MUX) is replaced by a power splitter/combiner [17], [18]. A power-splitter-based optical distribution network (ODN) is compatible with the currently used time TDM-PONs, thus the infrastructure currently being used can be directly employed to implement UDWDM-RoF-PONs, to further increase the data transmission capacity.

In this paper, we proposed and demonstrate, for the first time to the best of our knowledge, a RoF link employing coherent detection of an OSSB RoF signal. The system is transparent to the modulation format and the data rate, thus it is suitable for both the uplink and downlink transmission in a channel of a coherent UDWDM-RoF-PON. Specifically, at the transmitter, a light wave from a laser source is externally modulated by a real-valued pre-coded microwave vector signal via a dual-parallel Mach-Zehnder modulator (DP-MZM) to generate an OSSB RoF signal. At the output of the DP-MZM, the OSSB RoF signal is sent to a coherent receiver over a single-mode fiber (SMF), to detect the RoF signal, where an LO laser source is employed for coherent detection. A digital signal processing (DSP) algorithm is developed to recover the standard microwave vector signal from the real-valued pre-coded microwave vector signal while cancelling the phase noise and the unstable frequency difference introduced by both the transmitter laser source and LO laser source. The reason that the microwave vector signal is pre-coded is that the DSP algorithm will change the phase and amplitude of the microwave vector signal while cancelling the phase noise. To obtain a standard microwave vector signal, pre-coding the phase term and the amplitude term of the microwave vector signal is necessary. The proposed DSP-assisted coherent RoF system based on two free-running laser sources with OSSB modulation in a UDWDM-PON is verified by an experiment. In the experiment, a 2.5 Gbps OSSB RoF signal with a channel

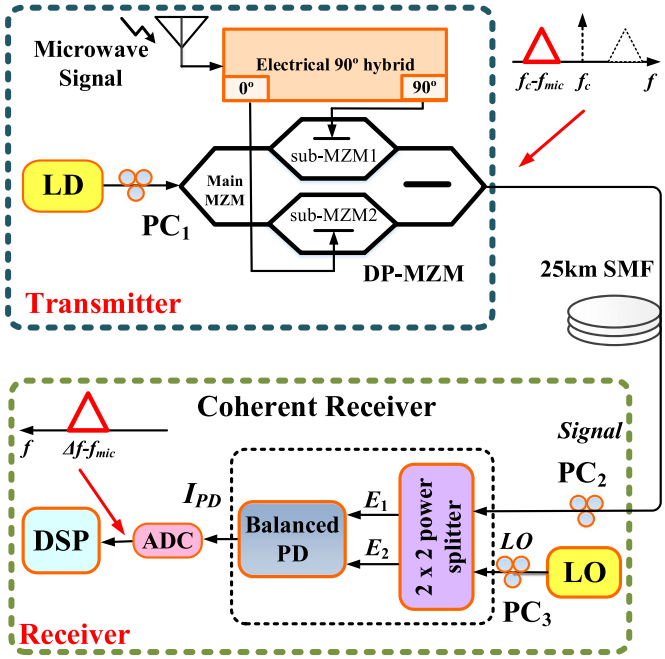

Fig. 2. Schematic diagram of the proposed RoF system based on the OSSB modulation employing coherent detection incorporating digital phase noise cancellation. ADC: analog-to-digital converter, PC: polarization controller, LD: laser diode, LO: Local oscillator, Balanced PD: balanced photodetector, DP-MZM: dual parallel Mach-Zehnder modulator, DSP: digital signal processing, fc: the center frequency of the light from LD, f_{mic}: the center frequency of the microwave signal, Δf: the frequency difference between LD and the LO laser source.

spacing as narrow as 3 GHz over a 25-km SMF link is demodulated. The channel selection is realized through coherent detection with a digital bandpass filter. For the transmission of a 2.5-Gbps 16 quadrature amplitude modulation (16-QAM) microwave vector signal, the optical sensitivity at the feed forward correction (FEC) level over a 25-km SMF link is −24.8 dBm, while for a 1.875-Gbps 8 phase shift keying (8-PSK) microwave vector signal, the optical sensitivity can reach −29.8 dBm which leaves an enough margin to accommodate the splitting losses in the ODN.

II. Principle of Operation

Fig. 2 shows the schematic diagram of the proposed DSP-assisted RoF system with coherent detection employing OSSB modulation. A continuous-wavelength (CW) light from a laser diode with the power P_s and the angular frequency ω_c is sent via a polarization controller (PC1) to a DP-MZM where it is externally modulated by a real-valued pre-coded microwave vector signal. The real-valued pre-coded microwave vector signal is applied to the DP-MZM via the two RF electrodes with one channel having a $\pi/2$ phase shift. The DP-MZM consists of two sub-MZMs (sub-MZM1 and sub-MZM2). Both sub-MZM1 and the sub-MZM2 are biased at the null transmission point while the main MZM is biased at the quadrature point. At the output of the DP-MZM, an OSSB signal without optical carrier is obtained which then is sent to a coherent receiver over a 25-km SMF [10]. At the coherent re-

ceiver, a free-running LO laser source is used as the LO laser source to detect the OSSB signal. A DSP algorithm is developed to recover the standard microwave vector signal from the real-valued pre-coded microwave vector signal while cancelling the phase noise and the frequency difference introduced by the transmitter laser source and LO laser source.

The optical field at the output of the DP-MZM can be written by

$$E_s(t) = \sqrt{2P_s}/2 \times \begin{bmatrix} \sin(\pi S_{RF}(t)/2V_\pi)\, e^{j(\omega_c t+\phi_c(t)+\pi/4)} \\ +\sin(\pi \hat{S}_{RF}(t)/2V_\pi) e^{j(\omega_c t+\phi_c(t)-\pi/4)} \end{bmatrix} \quad (1)$$

where $S_{RF}(t)$ is the real-valued pre-coded microwave vector signal, $S^{\wedge}_{RF}(t)$ is the Hilbert transform of the signal $S_{RF}(t)$, ω_c is the angular frequency and $\phi_c(t)$ is the phase of the light wave from the transmitter laser source, and V_π is the half-wave voltage of the DP-MZM.

Here, the real-valued pre-coded baseband vector signal is expressed as

$$\begin{aligned} &S_{\text{real-valued-baseband}}(t) = r_m \cos(\omega_s t + \theta_n) \\ &m = 1, 2, ..., M_1; \quad n = 1, 2, ..., M_2 \end{aligned} \quad (2)$$

The real-valued pre-coded baseband vector signal can be viewed as a signal with the combined amplitude (r_m) and phase (θ_n) modulation. $\{r_m, 1 \le \mathrm{m} \le \mathrm{M}_1\}$ denotes the set of M_1 possible amplitudes while $\{\theta_n, 1 \le \mathrm{n} \le \mathrm{M}_2\}$ is the M_2 possible phases of the carrier that convey the transmitted information [19]. ω_s is equal to the value of the symbol rate for the pre-coded baseband vector signal. Then, the real-valued pre-coded baseband vector signal is up converted to the microwave band. The real-valued pre-coded microwave vector signal $S_{RF}(t)$ can be written by

$$\begin{aligned} &S_{\mathrm{RF}}(t) = r_m \cos(\omega_s t + \theta_n) \cdot \cos(\omega_{\mathrm{RF}} t) \\ &m = 1, 2, ..., M_1; \quad n = 1, 2, ..., M_2 \end{aligned} \quad (3)$$

and the Hilbert transform of the signal $S_{\mathrm{RF}}(t)$ can be expressed as

$$\begin{aligned} &\hat{S}_{\mathrm{RF}}(t) = r_m \cos(\omega_s t + \theta_n) \cdot \sin(\omega_{\mathrm{RF}} t) \\ &m = 1, 2, ..., M_1; \quad n = 1, 2, ..., M_2 \end{aligned} \quad (4)$$

where ω_{RF} is the center frequency of the real-valued pre-coded microwave vector signal [20].

After the OSSB modulation, the optical signal at the output of the DP-MZM is sent to the receiver over an SMF. At the receiver side, a coherent receiver with a free-running LO laser source is used to coherently detect the OSSB RoF signal. The optical field of the light wave from the LO laser source is given by

$$E_{\mathrm{LO}}(t) = \sqrt{2P_{\mathrm{LO}}}\, e^{j(\omega_{\mathrm{LO}} t + \phi_{\mathrm{LO}}(t))} \quad (5)$$

where P_{LO} is the optical power and ω_{LO} is the angular frequency, and $\phi_{\mathrm{LO}}(t)$ is the phase term.

By tuning the two PCs (PC_2 and PC_3), the polarization direction of the OSSB RoF signal is adjusted to be parallel to the polarization direction of the light wave from the LO at the inputs of the 2×2 power splitter. At the two outputs of the 2×2 power splitter, the optical signals can be expressed as

$$E_1 = \sqrt{L_h}(\sqrt{L_s} E_s + E_{\mathrm{LO}}) \quad (6)$$

$$E_2 = \sqrt{L_h}(\sqrt{L_s} E_s - E_{\mathrm{LO}}) \quad (7)$$

where L_s is the link loss and L_h is the loss caused by the 2×2 power splitter.

Then, the two optical signals are applied to a balanced PD. The electrical signal at the output of the balanced PD can be written by

$$I_{\mathrm{PD}} = R(E_1 \cdot E_1^* - E_2 \cdot E_2^*)/2 = 2RL_h\sqrt{P_s P_{\mathrm{LO}} L_s} \times \begin{bmatrix} \sin(\pi S_{\mathrm{RF}}(t)/2V_\pi) \\ \times \cos(\Delta\omega t + \varphi_c(t) - \varphi_{\mathrm{LO}}(t) + \pi/4) \\ + \sin(\pi \hat{S}_{\mathrm{RF}}(t)/2V_\pi) \\ \times \cos(\Delta\omega t + \varphi_c(t) - \varphi_{\mathrm{LO}}(t) - \pi/4) \end{bmatrix} \quad (8)$$

where R is the responsivity of the balanced PD. If we assume that $S_{\mathrm{RF}}(t)$ is a small signal, (8) can be rewritten as

$$I_{\mathrm{PD}} \approx \frac{\pi R L_h \sqrt{P_s P_{\mathrm{LO}} L_s}}{V_\pi} \times \begin{bmatrix} S_{\mathrm{RF}}(t) \times \cos\begin{pmatrix} \Delta\omega t + \varphi_c(t) \\ -\varphi_{\mathrm{LO}}(t) + \frac{\pi}{4} \end{pmatrix} \\ + \hat{S}_{\mathrm{RF}}(t) \times \cos\begin{pmatrix} \Delta\omega t + \varphi_c(t) \\ -\varphi_{\mathrm{LO}}(t) - \frac{\pi}{4} \end{pmatrix} \end{bmatrix} \quad (9)$$

where $\Delta\omega$ is the frequency difference between the transmitter laser source and the LO laser source, $\Delta\omega = \omega_c - \omega_{\mathrm{LO}}$. Apparently, I_{PD} is an SSB signal [21]. Then, the electrical signal, I_{PD}, is sampled and digitized by an analog-to-digital converter (ADC). Using a DSP module, we can calculate the square of the sampled signal,

$$\begin{aligned} I_o &= I_{\mathrm{PD}}^2 \\ &= \pi^2 R^2 L_h^2 P_s P_{\mathrm{LO}} L_s / 4V_\pi^2 \times r_m^2 \cos(2\omega_s t + 2\theta_n) \\ &\quad + \pi^2 R^2 L_h^2 P_s P_{\mathrm{LO}} L_s / 4V_\pi^2 \times r_m^2 \\ &\quad - \pi^2 R^2 L_h^2 P_s P_{\mathrm{LO}} L_s / 2V_\pi^2 \times \left[r_m^2 \cos^2(\omega_s t + \theta_n)\right] \\ &\quad \times \left[\sin(2\Delta\omega t - 2\omega_{\mathrm{RF}} t + 2\varphi_c(t) - 2\varphi_{\mathrm{LO}}(t))\right] \end{aligned} \quad (10)$$

In (10), it can be seen that the first term is independent of both the phase noise and the frequency difference between the two laser sources, and it contains all the transmitted information. A digital bandpass filter can be used to extract the signal which is expressed as the first term in (10). Then, we have

$$I_1 = \pi^2 R^2 L_h^2 P_s P_{\mathrm{LO}} L_s / 4V_\pi^2 \times r_m^2 \cos(2\omega_s t + 2\theta_n) \quad (11)$$

Here the amplitude and phase information in (11) are r_m^2 and $2\,\theta_n$, respectively. Thus, the amplitude r_m and phase θ_n of the driving signal $S_{\mathrm{RF}}(t)$ must be pre-coded in order to obtain

TABLE I
THE POSSIBLE AMPLITUDES AND PHASES FOR THE PRE-CODED QPSK, 8-PSK AND 16-QAM SIGNALS

	Amplitudes (r_m)	Phases (θ_n)
QPSK	1	$\pi/8, 5\pi/8, 11\pi/8, 15\pi/8$
8-PSK	1	$+\pi/16, \pm5\pi/16, \pm9\pi/16, \pm13\pi/16$
16-QAM	1, $\sqrt{2}$	$\pm\pi/16, \pm5\pi/16, \pm9\pi/16, \pm13\pi/16$

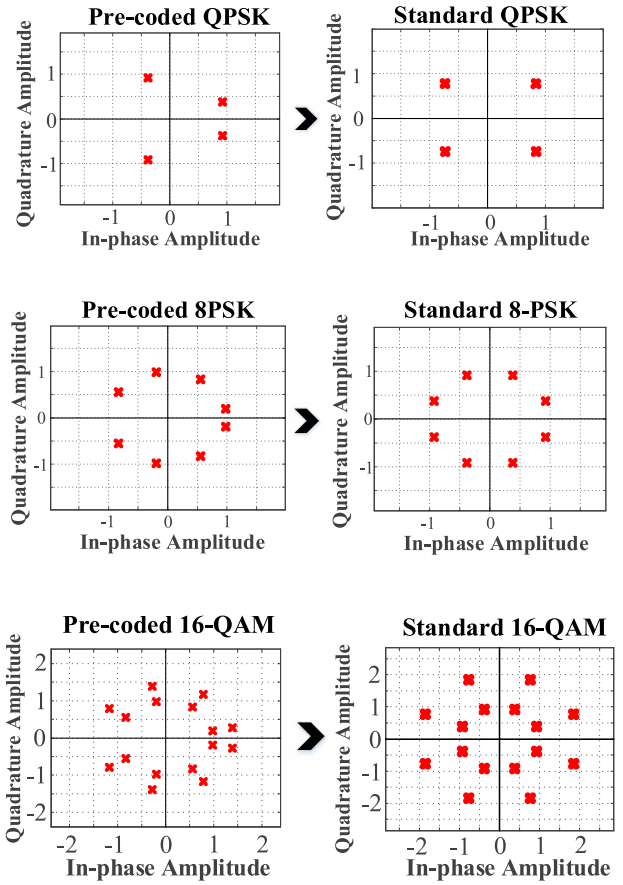

Fig. 3. The constellations for the pre-coded QPSK, 8-PSK, 16-QAM and the standard QPSK, 8-PSK, 16-QAM.

the standard vector signal at the receiver. Table I shows the possible amplitudes and phases for the pre-coded QPSK, 8-PSK and 16-QAM vector signals. Fig. 3 shows the constellations for the pre-coded vector signals (QPSK, 8-PSK and 16-QAM) and the standard vector signals (QPSK, 8-PSK and 16-QAM).

The phases of the pre-coded QPSK, 8-PSK and 16-QAM signals are half of the generated standard QPSK, 8-PSK and 16-QAM signals at the output of the DSP module and the amplitudes of the generated standard 16-QAM signal at the output of the DSP module are the square of the amplitudes of the pre-coded 16-QAM signal.

After the DSP module, the standard vector signal (QPSK, 8-PSK, 16-QAM) which is free from phase noise and unstable frequency difference introduced by the two laser sources is achieved.

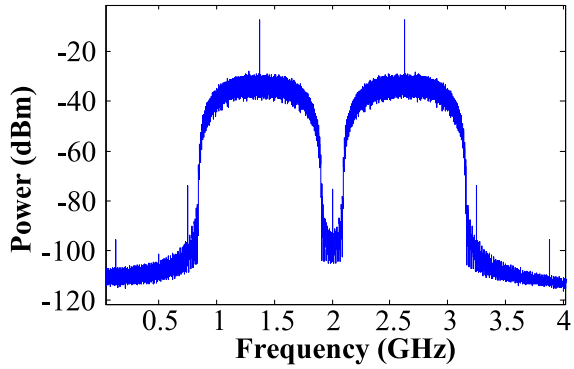

Fig. 4. Spectrum of the real-valued pre-coded 8-PSK microwave signal (Center frequency: 2 GHz, Symbol rate: 625 MSymbol/s, Bit rate: 1.875 Gbps).

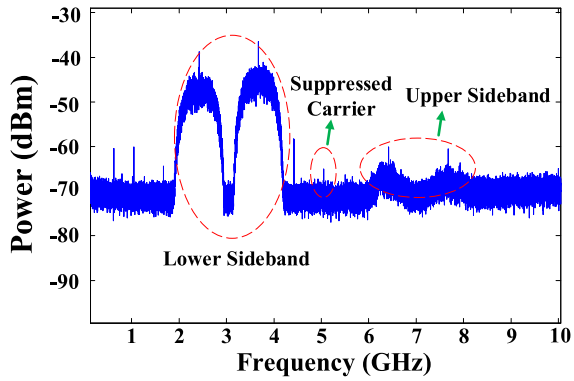

Fig. 5. Spectrum of the signal at the output of the coherent receiver.

III. EXPERIMENT

An experiment based on the setup shown in Fig. 1 is conducted. A CW light at 1549.947 nm from a tunable laser source (TLS, Agilent N7714A) with a linewidth of 100 KHz and an optical power of 16 dBm is sent to the DP-MZM (JDS-U) via PC_1. (Note that the polarization controller can be replaced by a polarization maintaing fiber). The half-wave voltage of the DP-MZM is about 6.33 V and the bandwidth is 10 GHz. A real-valued pre-coded microwave vector signal with a center frequency of 2 GHz and a symbol rate of 625 MSymbol/s generated by an arbitrary waveform generator (Tektronix AWG7102) is used to drive the DP-MZM via the two RF ports. A broadband electrical 90° hybrid (Crane Aerospace & Electronics, QHM-4R-9.5G) provides $\pi/2$ phase difference between the two drive signals. Both sub-MZM1 and sub-MZM2 in the DP-MZM are biased at the null transmission point while the main MZM is biased at the quadrature point. An OSSB RoF signal with no optical carrier is generated at the output of the DP-MZM (The suppression ratio for the optical carrier is about 30 dB, while the suppression ratio for the upper sideband is more than 20 dB), which is then transmitted over a 25 km SMF and coherently detected at the coherent receiver (Discovery Semiconductors DP-QPSK 40/100 Gbps Coherent Receiver Lab Buddy). A second CW light at 1549.988 nm with a linewidth of 700 KHz and an optical power of 7.8 dBm from a second TLS (Anritsu

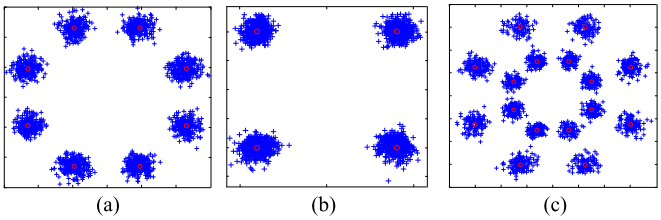

Fig. 6. The measured constellations for the recovered standard vector signals. (a) The standard 8-PSK signal (the received optical power: −23.8 dBm), (b) the standard QPSK signal (the received optical power: −23.8 dBm), (c) the standard 16-QAM signal (the received optical power: −24.9 dBm).

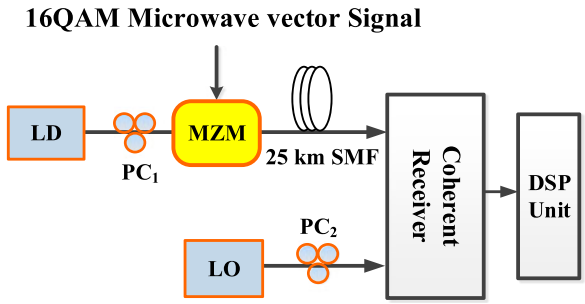

Fig. 7. Schematic diagram of an IM/CD RoF link without a PNC module and precoding.

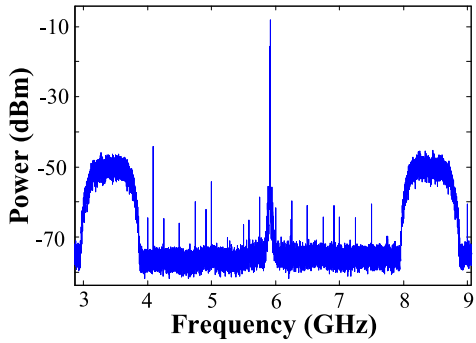

Fig. 8. Spectrum of the signal at the output of the coherent receiver for the IM/CD RoF link without precoding and a PNC module.

MG9638A) used as the LO laser source is applied to the coherent receiver via the LO port. The frequency difference between the transmitter laser source and the LO laser source is around 5.1 GHz. By tuning PC_2 and PC_3, the light wave from the LO laser source is co-polarized with the OSSB RoF signal. Note that in a practical system, we can use a polarization diversity receiver instead of tuning PC_2 and PC_3. At the output of the coherent receiver, a Digital Storage Oscilloscope (Agilent DSO-X 93204A) is employed to perform the analog-to-digital conversion with a sampling rate of 80 GSa/s to convert the electrical signal to a digital signal. Then, the digital signal (I_{PD}) is processed offline in a computer (Since the function of the DSP unit is just like an analog bandpass filter plus an analog envelope detector and a microwave vector signal demodulator, in order to avoid using a high sampling-rate analog to digital converter (ADC), in a practical system, the ADC can be replaced with these analog circuits).

First, we apply a real-valued pre-coded 8-PSK microwave vector signal with its spectrum is shown in Fig. 4 to the DP-MZM. The real-valued pre-coded 8-PSK microwave vector signal has a center frequency of 2 GHz and a symbol rate of 625 MSymbol/s or a bit rate of 1.875 Gbps. Fig. 5 shows the spectrum at the output of the coherent receiver. It can be seen that the detected real-valued pre-coded 8-PSK microwave vector signal (the signal with a center frequency of 3.1 GHz) in Fig. 5 is just the mixing product of the 2 GHz transmitted microwave vector signal and the 5.1 GHz electrical carrier whose frequency is just the frequency difference between the two laser sources. In addition, the 5.1 GHz electrical carrier and the upper-sideband signal are suppressed by more than 20 dB, which proves that an OSSB RoF signal with a bandwidth of around 3 GHz is successfully generated (If a bias voltage controller is employed for the DP-MZM, the leakages from both the optical carrier and upper sideband signal can be below the noise floor. So they will not affect other signals in other channels). After being digitized and processed in the DSP module to cancel both the phase noise and frequency difference between the two laser sources, a standard 8-PSK signal is obtained. The measured constellation for the recovered standard 8-PSK signal is shown in Fig. 6(a), when the received optical power is −23.8 dBm. Then, we also apply a real-valued pre-coded QPSK microwave vector signal with a bit rate of 1.25 Gbps and a real-valued pre-coded 16-QAM microwave vector signal with a bit rate of 2.5 Gbps to the DP-MZM, respectively. The symbol rates for the QPSK and 16-QAM signals are both 625 MSymbol/s and the center frequencies are 2 GHz. The measured constellations for the recovered standard vector signals are shown in Fig. 6(b) and (c). As can be seen, the constellations are very clear which again proves that the OSSB RoF signal is demodulated successfully. Since the function of the DSP module is just like the function of an envelope detector, the Gaussian white noise is higher for the vector signals that have larger amplitudes. That is the reason why in Fig. 6(c) the constellations at the outer circle are not as clear as those at the inner circle.

To verify the effectiveness of the proposed phase noise cancellation (PNC) technique, we also measure the constellations of the detected signal for a conventional intensity-modulation and coherent-detection (IM/CD) RoF link without using precoding and a PNC module. The experimental setup is shown in Fig. 7. Here, the microwave vector signal is a standard 16 quadrature amplitude modulation (16-QAM) signal with a center frequency of 2.5 GHz and a symbol rate of 625 MSymbol/s. The linewidth of the transmitter laser source is 100 kHz and the linewidth of the LO laser source is 700 kHz. The frequency stability for the transmitter laser source is ±0.3 GHz/24 hours, and for the LO laser source it is ±100 MHz/hour. The detected signal at the output of the coherent receiver is affected by the unstable frequency difference and the phase noise introduced by the two laser sources. A conventional digital phase lock loop is not able to track the unstable frequency difference between the two laser sources. Fig. 8 shows the spectrum of the signal at the output of the coherent receiver. After coherent detection

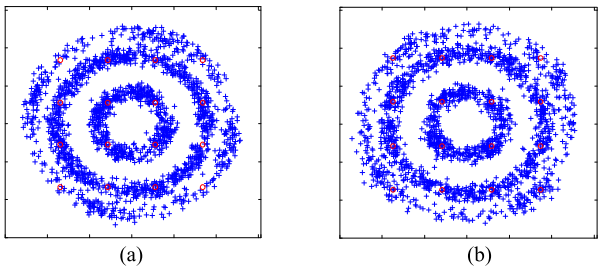

Fig. 9. The measured constellations of the signals at the output of the coherent receiver for an IM/CD RoF link. (a) The upper sideband signal, and (b) the lower sideband signal.

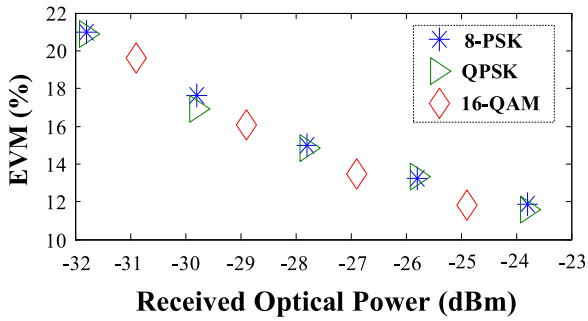

Fig. 10. EVM measurements at different received optical power levels for the recovered QPSK, 8-PSK and 16-QAM signals transmitted over a 25-km SMF.

and sampling, two digital bandpass filters are used to select the upper sideband signal and lower sideband signal. Then, the two signals are demodulated in the DSP unit. The constellations of the 16-QAM microwave signals (upper and lower sidebands) are shown in Fig. 9. As can be seen, the recovered 16-QAM microwave vector signals are strongly affected by the phase noise and the unstable frequency difference introduced by the two laser sources.

To further study the performance of the whole system, error vector magnitudes (EVMs) for the recovered standard vector signals (QPSK, 8-PSK and 16-QAM) versus the received Optical power levels are also measured, which are shown in Fig. 10. In Fig. 10, the symbol rates for the QPSK, 8-PSK and 16-QAM are all 625 MSymbol/s and the center frequencies for their corresponding real-valued pre-coded input microwave vector signals are 2 GHz. As can be seen, even the received optical power is only -31.8 dBm, the EVMs for the three different modulation-format vector signals can be still less than 21%.

Then, the bit error rates (BERs) are estimated based on the relationship between an EVM and a BER [22]–[26]. Here we assume that the noise after the DSP module is a stationary random process with Gaussian statistics. Fig. 11 shows BERs as a function of the received optical power calculated from the measured EVMs. For the recovered standard 8-PSK signal, when the received optical power is -29.8 dBm, the BER can reach 7.1×10^{-4}. When the received optical power is -24.9 dBm, for the 16-QAM signal, the BER is less than 1×10^{-3}. While for the QPSK signal, when the received optical is only -31.8 dBm, the BER is still less

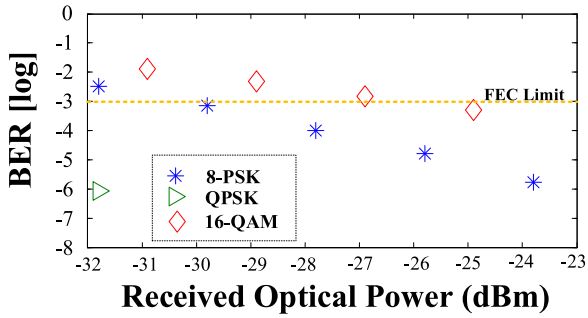

Fig. 11. BERs at different received optical power levels for the recovered QPSK, 8-PSK and 16-QAM signals transmitted over a 25-km SMF.

than 1×10^{-6}. By using a state-of-the-art FEC technique [27], error-free transmission can be achieved when a raw BER is less than 3×10^{-3}.

IV. Conclusion

An OSSB RoF system based on coherent detection for UDWDM-PONs was proposed and experimentally demonstrated. By proper pre-coding the input real-valued microwave vector signals and using a DSP algorithm, the real-valued microwave vector signals could be recovered. In the experiment, the phase noise and the unstable frequency difference introduced by the two free-running laser sources (the transmitter laser source and LO laser source) was cancelled through the DSP algorithm. Different modulation-format real-valued pre-coded microwave vector signals (1.25-Gbps QPSK, 1.875-Gbps 8-PSK and 2.5-Gbps 16-QAM) with center frequencies of 2 GHz were transmitted over a 25-km SMF and recovered at the coherent receiver. The channel spacing could be as narrow as 3 GHz and the date rate for each channel could reach 2.5 Gbps. The prosposed RoF link had a very high sensitivity. For the transmission of a 2.5-Gbps 16-QAM microwave vector signal over a 25-km SMF, the link had a sensitivity of -24.8 dBm (FEC level), while for a 1.875-Gbps 8-PSK microwave vector signal, the sensitivity could reach -29.8 dBm.

References

[1] A. J. Seeds, "Microwave photonics," *IEEE Trans. Microw. Theory Tech.*, vol. 50, no. 3, pp. 877–887, Mar. 2002.
[2] C. H. Cox III, E. I. Ackerman, G. Betts, and J. Prince, "Limits on the performance of RF-over-fiber links and their impact on device design," *IEEE Trans. Microw. Theory Tech.*, vol. 54, no. 2, pp. 906–920, Feb. 2006.
[3] J. Capmany and D. Novak, "Microwave photonics combines two worlds," *Nature Photon.*, vol. 1, no. 6, pp. 319–330, Jun. 2007.
[4] G. H. Smith, D. Novak, and Z. Ahmed, "Technique for optical SSB generation to overcome dispersion penalties in fibre-radio systems," *Electron. Lett.*, vol. 33, no. 1, pp. 74–75, Jan. 1997.
[5] G. H. Smith, D. Novak, and Z. Ahmed, "Overcoming chromatic-dispersion effects in fiber-wireless systems incorporating external modulators," *IEEE Trans. Microw. Theory Tech.*, vol. 45, no. 8, pp. 1410–1415, Aug. 1997.
[6] M. Xue, S. Pan, and Y. Zhao, "Optical single-sideband modulation based on a dual-drive MZM and a 120° hybrid coupler," *J. Lightw. Technol.*, vol. 32, no. 19, pp. 3317–3323, Oct. 2014.
[7] B. Hraimel, X. Zhang, Y. Pei, T. Liu, T, Xu, and Q. Nie, "Optical single-sideband modulation with tunable optical carrier to sideband ratio in radio over fiber," *J. Lightw. Technol.*, vol. 29, no. 5, pp. 775–781, Mar. 2011.

[8] Y. Zhang, F. Zhang, and S. Pan, "Optical single sideband modulation with tunable optical carrier-to-sideband ratio," *IEEE Photon. Technol. Lett.*, vol. 26, no. 7, pp. 653–655, Apr. 2014.
[9] J. L. Wei, X. Q. Jin, and J. M. Tang, "The influence of directly modulated DFB lasers on the transmission performance of carrier-suppressed single-sideband optical OFDM signals over IMDD SMF systems," *J. Lightw. Technol.*, vol. 27, no. 13, pp. 2412–2419, Jul. 2009.
[10] S. Shimotsu, S. Oikawa, T. Saitou, N. Mitsugi, K. Kubodera, T. Kawanishi, and M. Izutsu, "Single side-band modulation performance of a $LiNbO_3$ integrated modulator consisting of four-phase modulator waveguides," *IEEE Photon. Technol. Lett.*, vol. 13, no. 4, pp. 364–366, Apr. 2001.
[11] C. Lim, M. Attygalle, A. Nirmalathas, D. Novak, and R. Waterhouse, "Analysis of optical carrier-to-sideband ratio for improving transmission performance in fiber-radio links," *IEEE Trans. Microw. Theory Tech.*, vol. 54, no. 5, pp. 2181–2186, May 2006.
[12] X. Chen, T. Shao, and J. P. Yao, "Digital phase noise cancellation for a coherent-detection microwave photonic link," *IEEE Photon. Technol. Lett.*, vol. 26, no. 8, pp. 805–808, Apr. 2014.
[13] X. Chen and J. P. Yao, "A coherent microwave photonic link with digital phase noise cancellation," in *Proc. IEEE Int. Topical Meeting Microw. Photon. Conf.*, Oct. 2014, pp. 438–441.
[14] X. Chen and J. P. Yao, "Radio over colorless WDM-PON with wavelength reuse based on polarization multiplexing and coherent detection incorporating digital phase noise cancellation," presented at the *Opt. Fiber Commun. Conf. Exhib.*, Los Angeles, CA, USA, Mar. 22–26, 2015, Paper W1F.2.
[15] S. Camatel, V. Ferrero, R. Gaudino, and P. Poggiolini, "Optical phase-locked loop for coherent detection optical receiver," *Electron. Lett.*, vol. 40, no. 6, pp. 384–385, Mar. 2004.
[16] K. Kikuchi and K. Katoh, "Differential detection of single modulation sideband for ultra-dense optical frequency-division multiplexed systems," *Electron. Lett.*, vol. 38, no. 17, pp. 980–981, Aug. 2002.
[17] H. Rohde, E. Gottwald, A. Teixeira, J. D. Reis, A. Shahpari, K. Pulverer, and J. S. Wey, "Coherent ultra dense WDM technology for next generation optical metro and access networks," *J. Lightw. Technol.*, vol. 32, no. 10, pp. 2041–2052, May 2014.
[18] K. Grobe and M. Eiselt, *Wavelength Division Multiplexing: A Practical Engineering Guide*. Hoboken, NJ, USA: Wiley, 2014, pp. 271–273.
[19] J. G. Proakis and M. Salehi, *Digital Communications*, 5th ed. New York, NY, USA: McGraw-Hill, 2008, pp. 97–104.
[20] A. D. Poularikas, *The Handbook of Formulas and Tables for Signal Processing*. Boca Raton, FL, USA: CRC, 1999.
[21] L. W. Couch, *Digital and Analog Communication System*, 8th ed. Upper Saddle River, NJ, USA: Pearson, 2013, pp. 324–325.
[22] D. H. Wolaver, "Measure error rates quickly and accurately," *Electron. Des.*, vol. 43, no. 11, pp. 89–98, May 1995.
[23] A. Brillant, *Digital and Analog Fiber Optic Communication for CATV and FTTx Applications*. Bellingham, WA, USA: SPIE, 2008, pp. 653–660.
[24] V. J. Urick, J. X. Qiu, and F. Bucholtz, "Wide-band QAM-over-fiber using phase modulation and interferometric demodulation," *IEEE Photon. Technol. Lett.*, vol. 16, no. 10, pp. 2374–2376, Oct. 2004.
[25] J. Lu, K. B. Letaief, J. C.-I. Chuang, and M. L. Liou, "M-PSK and M-QAM BER computation using signal-space concepts," *IEEE Trans. Commun.*, vol. 47, no. 2, pp. 181–184, Feb. 1999.
[26] L. Hanzo, M. Münster, B. J. Choi and T. Keller, *OFDM and MC-CDMA for Broadband Multi-User Communications, WLANs and Broadcasting*. Hoboken, NJ, USA: Wiley, 2003, pp. 419–429.
[27] R. Schmogrow, D. Hillerkuss, S. Wolf, B. Bäuerle, M. Winter, P. Kleinow, B. Nebendahl, T. Dippon, P. C. Schindler, C. Koos, W. Freude, and J. Leuthold, "512QAM Nyquist sinc-pulse transmission at 54 Gbit/s in an optical bandwidth of 3 GHz," *Opt. Exp.*, vol. 20, no. 6, pp. 6439–6447, Mar. 2012.

Xiang Chen (S'13) received the B.Eng. degree in communications engineering from Donghua University, Shanghai, China, in 2009, and the M.Sc. degree in communications and information engineering from Shanghai University, Shanghai, in 2012. He is currently working toward the Ph.D. degree in electrical and computer engineering at the Microwave Photonics Research Labstoratory, School of Electrical Engineering and Computer Science, University of Ottawa, Ottawa, ON, Canada.

His current research interests include coherent radio-over-fiber systems and the dynamic range of analog optical links.

Jianping Yao (M'99–SM'01–F'12) received the Ph.D. degree in electrical engineering from the Université de Toulon et du Var, La Garde, France, in December 1997.

He is currently a Professor and the University Research Chair in the School of Electrical Engineering and Computer Science, University of Ottawa, Ottawa, ON, Canada. From 1998 to 2001, he was with the School of Electrical and Electronic Engineering, Nanyang Technological University, Singapore, as an Assistant Professor. In December 2001, he joined the School of Electrical Engineering and Computer Science, University of Ottawa, as an Assistant Professor, where he became an Associate Professor in 2003, and a Full Professor in 2006. He was appointed the University Research Chair in Microwave Photonics in 2007. From July 2007 to June 2010, he was the Director of the Ottawa-Carleton Institute for Electrical and Computer Engineering. He was reappointed Director of the Ottawa-Carleton Institute for Electrical and Computer Engineering in 2013. He has authored or co-authored more than 510 research papers, including more than 300 papers in peer-reviewed journals, and 210 papers in conference proceedings. He is a Topical Editor for *Optics Letters*, and serves on the Editorial Boards of the IEEE TRANSACTIONS ON MICROWAVE THEORY AND TECHNIQUES, *Optics Communications*, *Frontiers of Optoelectronics*, and *Science Bulletin*. He was as a guest co-editor for a Focus Issue on Microwave Photonics in *Optics Express* in 2013 and a lead-editor for a Feature Issue on Microwave Photonics in *Photonics Research* in 2014. He is a Chair of numerous international conferences, symposia, and workshops, including the Vice Technical Program Committee (TPC) Chair of the IEEE Microwave Photonics Conference in 2007, TPC Co-Chair of the Asia-Pacific Microwave Photonics Conference in 2009 and 2010, TPC Chair of the high-speed and broadband wireless technologies subcommittee of the IEEE Radio Wireless Symposium in 2009–2012, TPC Chair of the microwave photonics subcommittee of the IEEE Photonics Society Annual Meeting in 2009, TPC Chair of the IEEE Microwave Photonics Conference in 2010, General Co-Chair of the IEEE Microwave Photonics Conference in 2011, TPC Co-Chair of the IEEE Microwave Photonics Conference in 2014, and General Co-Chair of the IEEE Microwave Photonics Conference in 2015. He is also a committee member of numerous international conferences, such as International Photonics Conference, Optical Fiber Communication, Bragg Gratings, Photosensitivity, and Poling in Glass Waveguides, and Meeting on Microwave Photonics. He is currently an IEEE MTT-S Distinguished Microwave Lecturer for 2013–2015.

Dr. Yao is a Registered Professional Engineer of Ontario. He is a Fellow of the Optical Society of America and the Canadian Academy of Engineering. He received the International Creative Research Award of the University of Ottawa, in 2005; the George S. Glinski Award for Excellence in Research, in 2007; and the Natural Sciences and Engineering Research Council of Canada Discovery Accelerator Supplements Award, in 2008. He was selected to receive an inaugural OSA Outstanding Reviewer Award in 2012.